Journal of Wind Engineering & Industrial Aerodynamics 169 (2017) 128–138

Contents lists available at ScienceDirect

Journal of Wind Engineering & Industrial Aerodynamics

journal homepage: www.elsevier.com/locate/jweia

Nonlinear dynamics of guyed masts under wind load: Sensitivity to structural parameters and load models

Jorge S. Ballaben [a,b], Alberto M. Guzmán [c], Marta B. Rosales [a,b,*]

[a] Departamento de Ingeniería, Universidad Nacional del Sur, Av. Alem 1253, 8000, Bahía Blanca, Argentina
[b] CONICET, Argentina
[c] CeReDeTeC, FRM, Universidad Tecnológica Nacional, Rodríguez 273, 5500, Mendoza, Argentina

ARTICLE INFO

Keywords:
Guyed mast
Guy tension
Dynamic response
Wind

ABSTRACT

As the wireless communications spread, there is an increasing demand of antenna supporting structures. Guyed lattice towers (masts) are chosen for economical reasons when there is enough space for their location. Radio and television industries employ structures that can attain heights up to 600 m and communication towers for mobile phones are approximately 60 m though higher structures are also constructed. For the latter, guyed masts are indicated. Nowadays, the demand for more accurate and reliable communication systems poses more stringent structural requirements since to attain high quality in signal transmission, small magnitude motions of the supporting structures are usually needed. The design of these structures is, in general, carried out following the standard codes and simplified models. Despite the large potential of adverse impact, the dynamic actions as wind and earthquakes, are not usually addressed in detail with exception of special cases. In this work, a parametric study on the effect of three relevant parameters (i.e. guy pretension, structural damping, mast stiffness) on a guyed mast is carried out. A typical structure under wind load is analyzed using a finite element model. Two load representations are employed; the mean component is obtained following procedures from standards and is the same for both load models. The fluctuating part of the wind load is then added. In the first model, the turbulent component is represented by a time series obtained by means of the Spectral Representation Method including temporal and spatial correlations. The second model is a simpler approach, in which the temporal component of the wind load is represented through a harmonic function. The resulting transverse displacements and cable tensions histories are analyzed to assess the dynamic structural response. It is observed that the structure is more sensitive to the guy pretension when compared with the other two variable parameters. Also, it was verified that the stochastic load is a more adequate option to model the wind. These two findings are crucial in the design of this type of structures.

1. Introduction

For many years, guyed masts have been used to support antennas for radio, TV and other communication signals. These structures have clear advantages in the open country where there are no restrictions on the position of the cable anchors. Sometimes they are also found in urban areas due to the low cost compared with other typologies. A typical configuration comprises of a lattice mast with triangular cross-section (three legs, horizontal and diagonal members) and several levels of guys (see Fig. 1). The height is variable depending on the application but nowadays it is not exceptional to see 300 m-high towers. The main structural characteristics are the large slenderness of the mast and the taut guys. Dynamic actions are, in general, assumed as quasi-static loads that represent the mean of the dynamic phenomena amplified with factors that account for the dynamics characteristics, following standard codes and recommendations. Since wind loads are essentially dynamic, a strong interaction with this flexible system can be expected.

Research on this subject includes works by Kahla (1993) who employs equivalent beam methods in order to simplify five lattice masts and carries out a static analysis. Wahba et al. (1998) and Madugula et al. (1998) evaluate the behavior of guyed towers and use the finite element method (FEM) to model the mast as a lattice and an equivalent beam-column. They study the influence of ice accretion, guy initial tensions and outriggers (torsion resistors) on the dynamic response of the structure. A finite difference approximation and FEM is proposed by Kewaisy (2001). The dynamics of cable supported structures using a

* Corresponding author. Departamento de Ingeniería, Universidad Nacional del Sur, Av. Alem 1253, 8000, Bahía Blanca, Argentina.
E-mail addresses: jorgeballaben@gmail.com (J.S. Ballaben), mguzman@frm.utn.edu.ar (A.M. Guzmán), mrosales@criba.edu.ar (M.B. Rosales).

http://dx.doi.org/10.1016/j.jweia.2017.07.012
Received 10 April 2017; Received in revised form 16 June 2017; Accepted 18 July 2017

Fig. 1. Typical guyed mast.

generalized FEM is addressed by Desai and Punde (2001). In this work, the free and forced responses of a simple guyed tower model show the efficiency of the approach with a few number of degrees of freedom. An interesting work was reported by Preidikman et al. (2006) in which the dynamic response of guyed masts using different models for cables is tackled. The variation of the stiffness of the complete system using different levels of pretension on the guys is evaluated. Meshmesha et al. (2006) study a guyed tower subjected to static and seismic loadings through an equivalent beam-column analysis based on a thin plate equivalence for lattice structures. The FEM was also employed to solve the dynamics of guyed towers by Shi (2007) and de Oliveira et al. (2007). Lu et al. (2010) employ the principle of harmonic wave superimpose method for the wind velocity simulation, as well as an improved approach that introduces the Fast Fourier Transform (FFT) to simulate the wind velocity time series along the height of a guyed mast. A study regarding the issue of the assessment and structural rehabilitation of a guyed mast was published by Saudi (2014).

In the present work, the dynamics of a guyed mast under the action of wind loads is evaluated. The aim of the study is to analyze the sensitivity of the structural response to changes in three relevant parameters. The lattice mast is modeled with an equivalent beam-column and the guys are represented by nonlinear prestressed cables. The selected parameters are the guy pretension, the structural damping and the mast stiffness. The guy pretension is known to be a critical variable in guyed systems and its impact can be significant to the structure behavior. An appropriate structural damping model is generally a controversial issue and its influence is also assessed in this study. Finally, the need of rehabilitation of this type of structures sometimes leads to a change in the mast stiffness which effect is also evaluated in the present work. The governing system is discretized using FEM, in particular using the software package Algor (Autodesk Inc., 2009). The fluctuating part of the stochastic wind load is found using the Spectral Representation Method (SRM), presented by Shinozuka and Jan (1972). With this methodology, it is possible to account for the spatial and temporal correlations. This load model is used by Venanzi et al. (2015) in a optimization study of cable-stayed masts. In the present work and for the sake of comparison, a simpler approach is used in which the wind dynamics is reproduced by a harmonic function. The statistical analysis of the outcomes allows to conclude that the guyed mast under wind action is more sensitive to the variation of the initial pretension, among all the considered parameters.

2. Structure description and fem modeling

The structure studied in this paper is a typical guyed mast (addressed also by Desai and Punde (2001)) 120 m tall, with four guy levels separated by 30 m, three guys at each level, oriented in vertical planes separated by 120° and two sets of guy anchors contained in each of the three planes (see Fig. 2).

The finite element software ALGOR (Autodesk Inc., 2009) is used to model the structure and solve the nonlinear dynamic problem in the time domain. The mast, fixed at the base, is modeled using an equivalent beam-column with twelve 6-DOF beam elements. Each guy is approximated using twenty 3-DOF two-node pretensioned truss elements. For both element types, large displacements are allowed. The material properties and parameter values used in this work are listed in Table 1. The label "standard case" (SC) denotes the reference case and it is highlighted in bold font.

2.1. *Sensitivity studies*

For various reasons, a guyed mast may suffer changes from its original design. Sometimes, there is public opposition to install antenna supporting structures due to potential environmental effects. This limitation can give place to the installation of new antennas and ancillaries by the structure owner and even the same structure could be shared by more than one company. Usually, some type of reinforcement must be implemented, say changes in the guy tensions, leg reinforcements, etc. A study of these changes impact on the dynamic response is presented herein. Also, since the literature suggests a wide range of values for the damping ratio, this coefficient is within the considered parameters.

2.1.1. *Initial pretension of the guys IP*

As mentioned before, the design guy pretension values may be modified due to some type of retrofitting. Also, the pretension can change during the service life of the structure due to temperature effects, failure of the guy anchors, etc. The initial pretension is given by the tensile force per area of the guys that is needed to attain the desired structural system stiffness. For design purposes, the standard code ANSI/TIA-222-G (ANSI/TIA-222-G, 2009) sets the pretension in a range of 7–15% of the ultimate breaking strength of the guys. In several situations, the initial pretension does not match the design value and may even be out of the recommended range and the whole structure behavior can be compromised. This work is intended to cover the range proposed by the standards. Based on the cross section and material of the guys assumed in the present study, the adopted values of initial pretension (as a force in kN) are 15, 20, 25, 30, 35 kN.

2.1.2. *Equivalent structural damping D*

Rayleigh damping is a usual approach in structural dynamics. Since it attempts to model the real damping of the structure, the use of an appropriate damping coefficient is necessary. As is known, the mass and stiffness coefficients are proportional to two natural frequencies of the structure. In order to obtain them, two steps are followed. First, the initial tension of the cables and the self-weight are applied within a static analysis from which a nonlinear equilibrium configuration is obtained. Second, this deformed configuration is adopted as the new geometry of the structure over which a linear frequency analysis is performed. Harikrishna et al. (2003) found, from experimental measures on a lattice guyed mast, values in the range of 1–3% of the critical damping. The International Association for Shell and Spatial Structures (International Association for Shell and Spatial Structures, 1991) recommends a 3% for bolted unions, the Argentinian standard code CIRSOC (CIRSOC-INTI, 2008), a 2%. It is observed that the values are included in a 1–3% range. In this paper, three values of the Rayleigh damping are considered: 1%, 2% and 3% of the critical damping. The proportional coefficients for the mass and stiffness matrix (*e.g.* Clough and Penzien (1993)) result 0.118 and 0.00070, 0.237 and 0.00144 and, 0.356 and 0.00209, for each

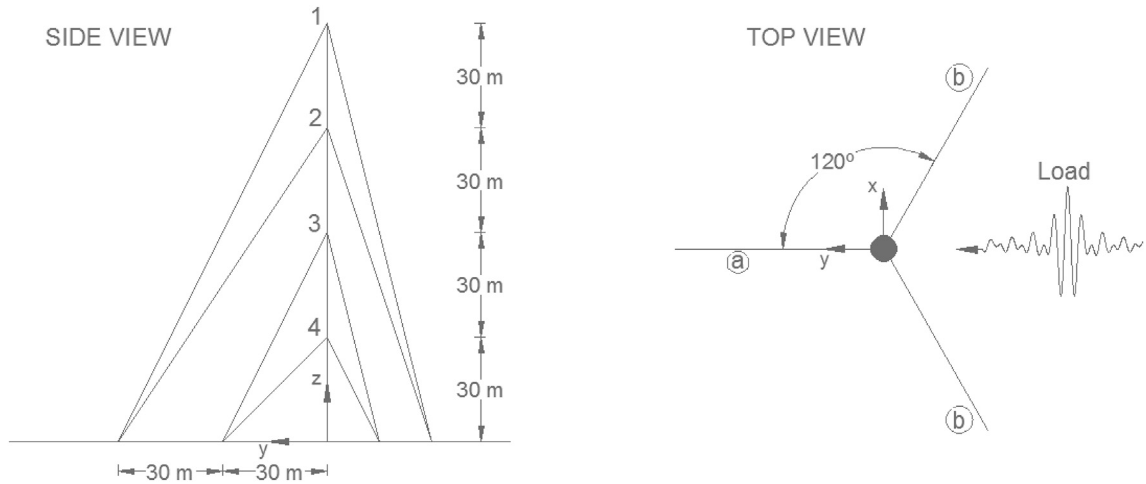

Fig. 2. Guyed mast geometry.

Table 1
Values of materials properties and parameters of the guyed mast. The "standard case" (SC) values are highlighted in bold font.

Properties	Unit	Value	Description
E_b	GPa	210	Column Young modulus
I	$m^4 \times 10^{-3}$	**1.8**, 2.25, 2.70	Column second area moment
σ	MPa	240	Column yield strength
A_b	$m^2 \times 10^{-3}$	1.98	Column area
m_b	kg/m	61	Column mass per unit length
E_c	GPa	150	Cable Young modulus
σ_u	MPa	1200	Cable ultimate strength
A_c	$m^2 \times 10^{-4}$	2	Cable area
m_c	kg/m	2.55	Cable mass per unit length
IP	kN	15, 20, **25**, 30, 35	Cable initial tension
D	%	1, **2**, 3	Rayleigh structural damping ratio
T_1	s	2.66	Fundamental period of the structure

damping level, respectively.

2.1.3. Mast bending stiffness I

The mast (tower) bending stiffness is set at the design stage. However, the need to change or incorporate new equipment in the structure could lead to eventual reinforcements. Thus, the design value of the bending stiffness can be modified through the modification of the second moment of the area of the mast cross section (I). In this work, the values 0.0018, 0.00225 and 0.0027 m^4, are assumed for I.

3. Dynamic loads

In order to simulate typical load conditions, three loads are taken into account: weight (gravitational load), pretension on the cables and dynamic lateral loads on the mast in the y direction (which defines an axis of symmetry in the arrangement of cables, see Fig. 2). Only displacements on the y direction will be reported. At this stage, no wind loads are applied on the guys.

3.1. Wind load

The wind loads used in the present study are described in detail in Appendix A. The load is calculated as a sum of a mean value and a fluctuating part. The mean component of the wind load is obtained in Appendix A.1 following the methodology proposed in the Argentinian standard (CIRSOC-INTI, 2005) (based on the ASCE-7 standard (American Society of Civil Engineers, 1998)). The fluctuating part of the wind load is modeled applying the Spectral Representation Method (Shinozuka and Jan, 1972) (SRM) in combination with the power spectrum for the wind proposed by Davenport (Dyrbye and Hansen, 1994) and an exponential type coherence function. These functions as well as all the necessary derivations are included in Appendix A.2. Alternatively and for the sake of comparison, a simple approach which is attained by a sum of cosine functions is included (Appendix A.3). The stochastic load will be referred as WL1 and the harmonic load as WL2.

3.2. Load application

The pretension is applied to the guys at $t = 0$ s and holds during the whole analysis. Gravity is set with a linear increase starting in a null value to the standard value in 3 s, and remains constant during the experiment. The wind load is applied starting at 4 s to the end of the calculation, to avoid transient effects due to the sudden application of the pretension.

The total time of the analysis is 400 s and the sampling rate is 10 Hz, considering that $T_1 = 2.66$ s. The time step in the numerical solver is adaptive in order to attain the convergence more efficiently.

4. Results

Next, the results are described and discussed. The displacements of the guyed mast are dealt with first and then, the dynamic cable tension is analyzed. In all cases, the reference parameter combination (SC) is 2% - 1.8×10^{-3} m^4–25 kN (as stated in Table 1) for the Rayleigh damping ratio (D), mast stiffness (proportional to the second moment of the cross sectional area of the mast I) and initial pretension (IP), respectively. In all the parametric sensitivity plots (unless otherwise indicated), the parameters are varied one at a time (D, I or IP), and the values of the other parameters are fixed at the standard case SC.

4.1. Displacements of the guyed mast

In what follows, the first 10 s of the response are discarded to avoid the effect of the transients due to the loads application. All the considered displacements are evaluated in the y direction (see Fig. 2) along which the largest displacements occur. A typical top displacement time history found with both approaches used to model the wind load, is shown in Fig. 3. The differences among them are apparent. The WL2 model yields a periodic motion that almost copies the load shape, particularly when the maximum amplitudes occur. This periodic behavior is also noticeable when the parameter sensitivity is studied. On the other hand, the WL1 model conduces to a nonperiodic motion which randomness derives from the stochastic formulation of the load.

A FFT study of the top displacements is depicted in Fig. 4. Even when the relevant frequencies of both approaches to model the wind load are the same, the nature (either stochastic or harmonic) of each formulation

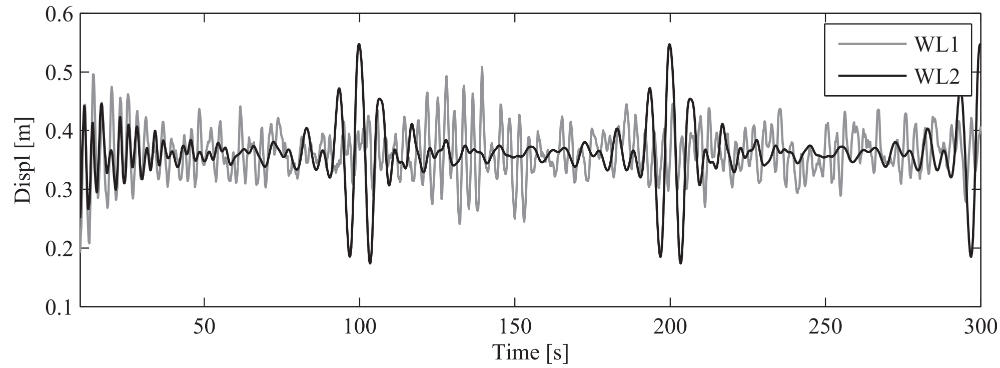

Fig. 3. Time history of the displacement at 120 m.

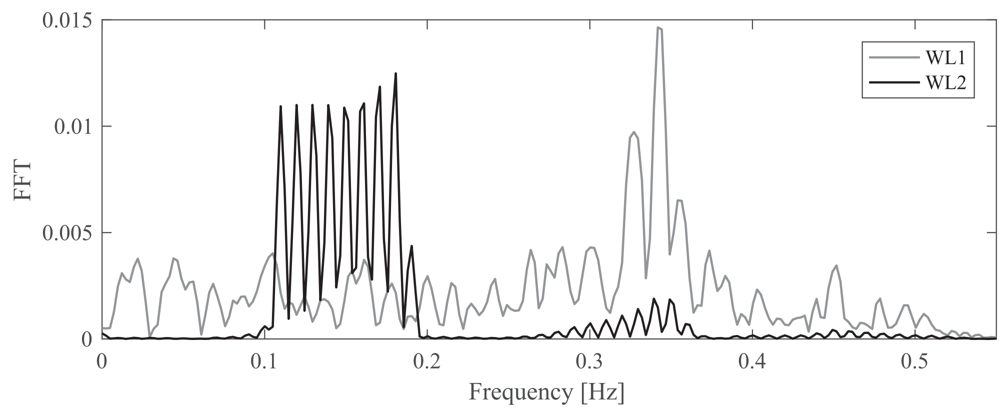

Fig. 4. FFT of the top displacement records.

is visible in the frequency content of the results. The highest peaks in the results found with WL2 correspond exactly with the peaks of the harmonic load, as expected, following the periodic behavior observed in Fig. 3. The results obtained with WL1 exhibit a larger content of frequencies and higher peaks that do not match neither the wind spectrum highest energy zone nor the natural frequencies of the structure. Both results observed in Figs. 3 and 4 for WL1 are a consequence of the interaction of the stochastic wind load and the nonlinear structure.

Next, the parameter sensitivity of the structural response is analyzed. Fig. 5 shows the results obtained varying the Rayleigh damping ratio (D), through three statistical measures of the displacement records (mean, 95% probability value and absolute maximum) at the top of the mast. When WL1 is used (Fig. 5a), D seems to have some small influence on the 95% and the maximum values. On the other hand, when WL2 is applied (Fig. 5b), there are no observable changes in the response due to the variation of D. Also, the maximum results predicted using WL2 are periodic and much higher than the obtained with WL1. It can be seen that the approach for modeling the loads affects directly the structural response sensitivity.

Since WL1 is a random load, the structural response is stochastic. The probability distributions functions (PDFs) of the displacements when D is varied are plotted in Fig. 6. All the resulting PDFs are Gamma-like and with very similar support, mode and dispersion (although small differences can be observed for $D = 1\%$). This clearly indicates that D, within the range of the herein studied values, has a small influence on the statistics of the response.

Next, the mast bending stiffness *E*I is varied (assuming a constant value of *E*) and the results evaluated at the top of the mast are depicted in Fig. 7.

In this case, the same influence is obtained for both load models and, contrary to the expected results, the increase in the mast stiffness leads to higher displacements. As is known, in a linear structure, an increase in the stiffness leads to a reduction in the structural displacements. In the present case, the interaction between the dynamic load and the nonlinear structure, conduces to the opposite result at the top of the mast. This is a significant aftermath. In effect, retrofitting (*e.g.* by means of reinforcements in the column legs) to reduce the motion of the mast is a common practice but, in the light of the present results, it could lead to the contrary outcome. This trend affects the three studied statistic measures (mean, 95% and absolute maximum values).

The PDF of the results at the top of the mast, with WL1 and varying I are depicted in Fig. 8. It can be seen that the resulting PDFs are similar in shape, size and support and the only differences among them is the shift to the right (higher displacements) observed when I is increased. These results allow to conclude that the mast stiffness affects (negatively), not only to the maximum displacement but also the complete record.

Finally, the results of the top displacements for both load models varying the initial tension of the guys (IP) are analyzed. The same statistical measures are plotted in Fig. 9. It can be seen that IP has a strong influence on the response, in terms of visible changes in the results and comparatively, with respect to the other studied parameters. The observed changes follow nonlinear paths, as expected, since the cables are the main cause of the nonlinear response of the structure.

The differences found among the results using the two load models are consistent with the previous outcomes: WL2 gives place to larger maximum displacements and, in this case, also slightly larger 95% displacements can be observed. The mean response is approximately the same using both load models.

The PDF of the displacements at the top of the mast applying WL1 and varying IP is depicted in Fig. 10. All the resulting PDFs are Gamma-like as in the previous cases, but the influence of IP is much larger. The support, mode and dispersion of the PDFs increase noticeably when the value of IP is decreased (i.e. lower IP values give much more disperse, higher and less predictable displacements).

From the previous studies, it can be concluded that IP is the most influential in both the dynamic and statistical responses and thus, is the

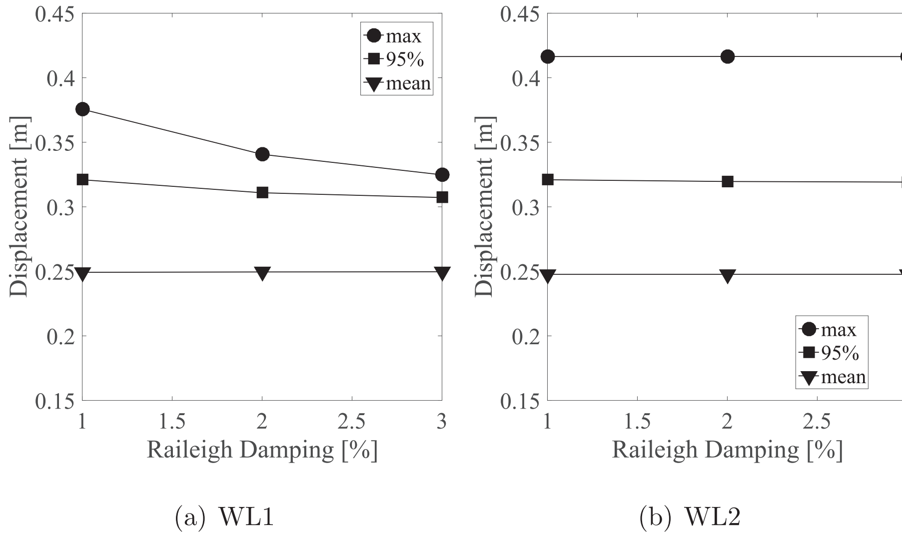

Fig. 5. Analysis of top displacements varying D (structural damping coefficient) with both load models.

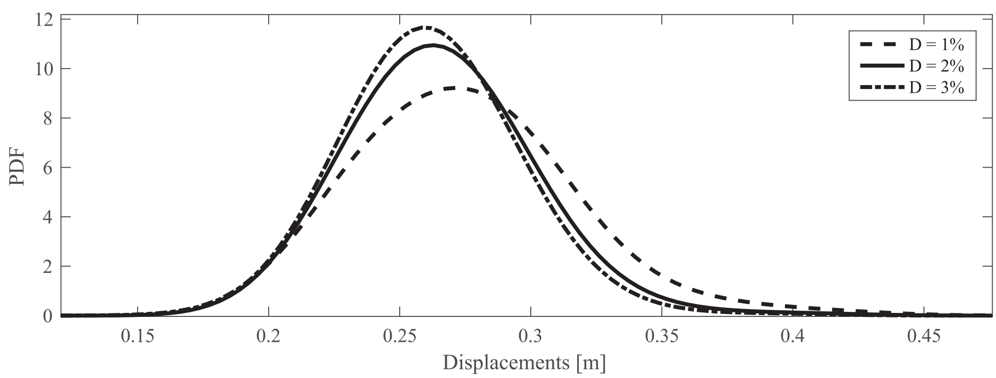

Fig. 6. PDF of the top displacements records using WL1 D (structural damping coefficient).

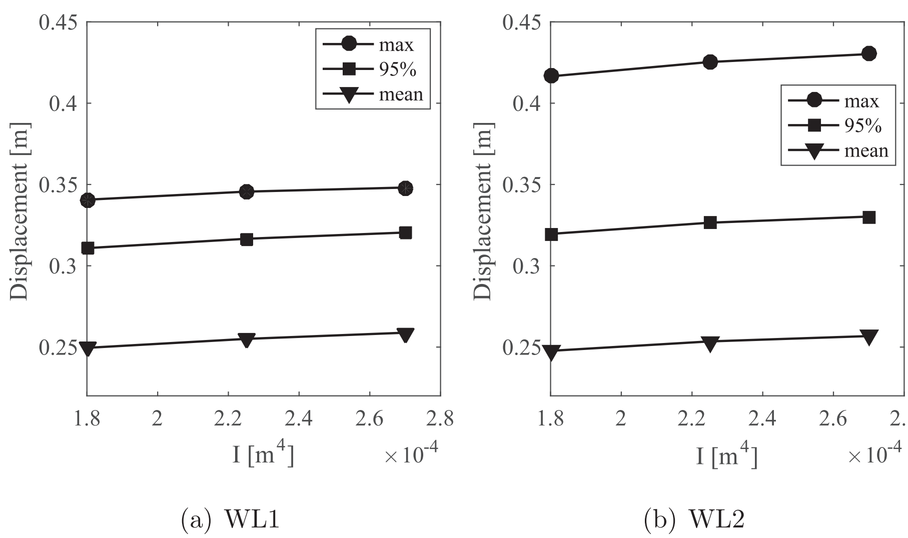

Fig. 7. Top displacements obtained varying the mast stiffness with both load models.

most relevant structural parameter of the ones herein studied.

Fig. 11 illustrates the impact of the parameters on the 95% probability values along the height (the portion from 60 m to the top of the mast). Fig. 11a depicts the effect on the absolute values. The IP remains the most important parameter at different heights. These values are also shown in Fig. 11b as percentages of the response found with the reference case. When the IP is lowered 40% (i.e., IP = 15 kN), the response is approximately 40% larger (the intermediate cases of 20 and 30 kN are not shown). Instead, when IP is increased 40%, the response decreases in 25% approximately. Thus, the effect on the guyed mast behavior when the IP is decreased or increased is not the same. The observed nonlinear behavior is due the interaction between the mast and the nonlinear

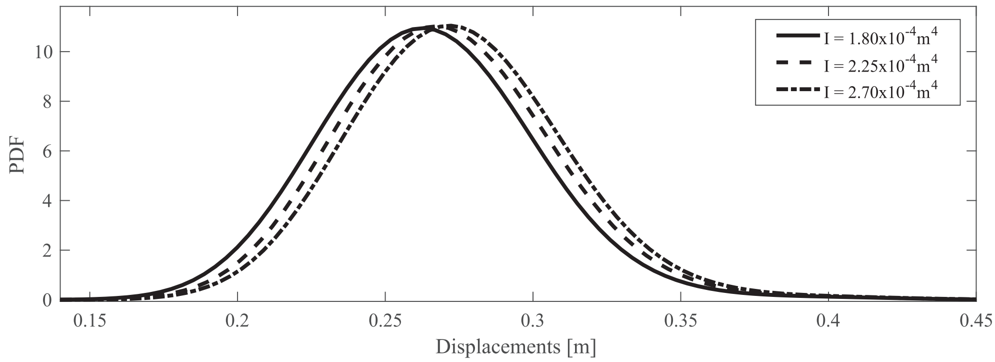

Fig. 8. PDF of the top displacements records WL1 varying the mast stiffness.

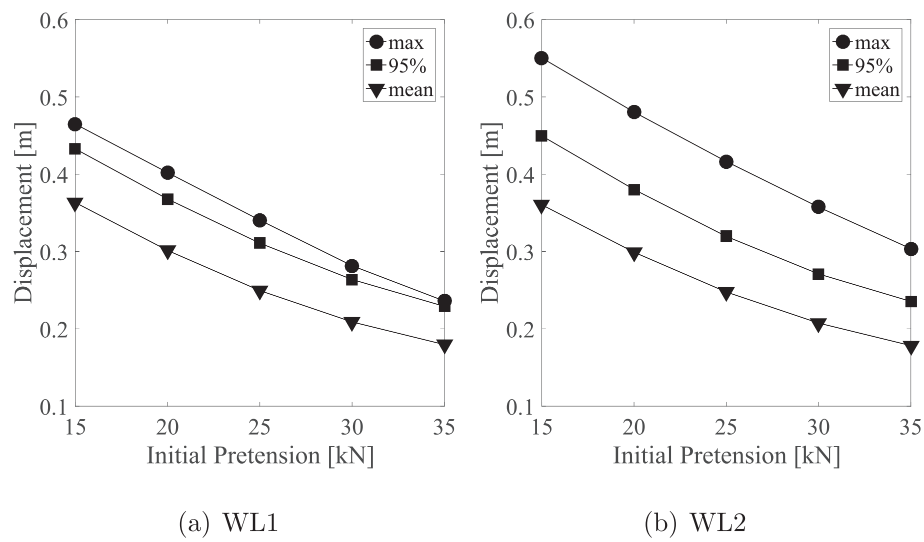

Fig. 9. Top displacements obtained varying the initial tension with both load models.

cables. This is relevant from an engineering viewpoint. Fig. 11c shows a zoomed view of Fig. 11b. Two conclusions can be drawn. The impact of both parameters (D and I) barely attains the 5%, and their influences are extremely variable with the height. Similar results are obtained for the maximum displacements; the mean values also exhibit results in a similar fashion for IP and I, while D does not seem to affect this magnitude.

When using the WL2 model, there are no changes along the height regardless the variation of the three parameters (WL2 is fully correlated along the height). From these conclusions, one infers that the chosen model for the wind load affects significantly the response. Recall that the *WL2* case leads to a harmonic function. Instead, the *SRM* employed to obtain the WL1 load covers all the range of frequencies of the spectrum and allows to model with more detail the dynamics of the wind velocity (including temporal and spatial correlations) allowing a better understanding of the real dynamic behavior of the guyed masts. Then, the load models become an important variable in the study of sensitivity, uncertainty quantification or optimization of these structures.

4.2. Guys tension

The variation of the guy tension during the dynamic event using WL1 is now discussed. The tension on the guys is an important design variable. The guys contribute strongly to the stiffness of the structure. More, the anchor points of the guys at the mast divide the length of the mast in segments reducing its buckling length. The outcomes will be presented as the PDF of the dynamic cable tension indicated as percentage of IP. Only IP is varied here, since is the only parameter of interest in the present issue.

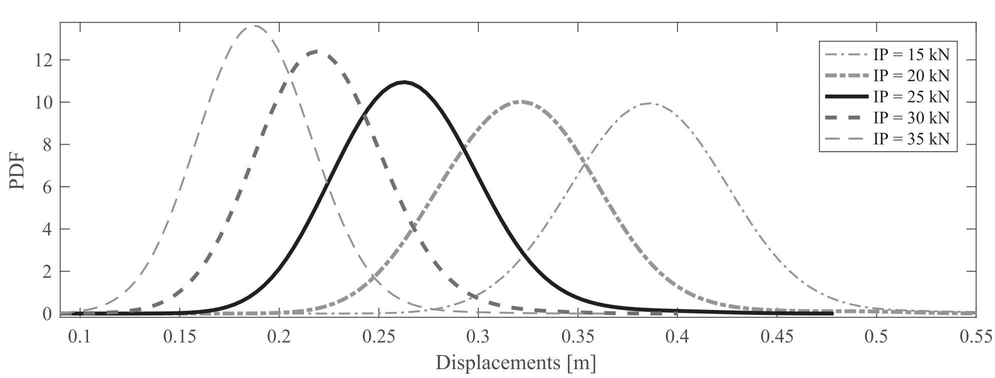

Fig. 10. PDF of the top displacement records using WL1 varying the guys initial pretension.

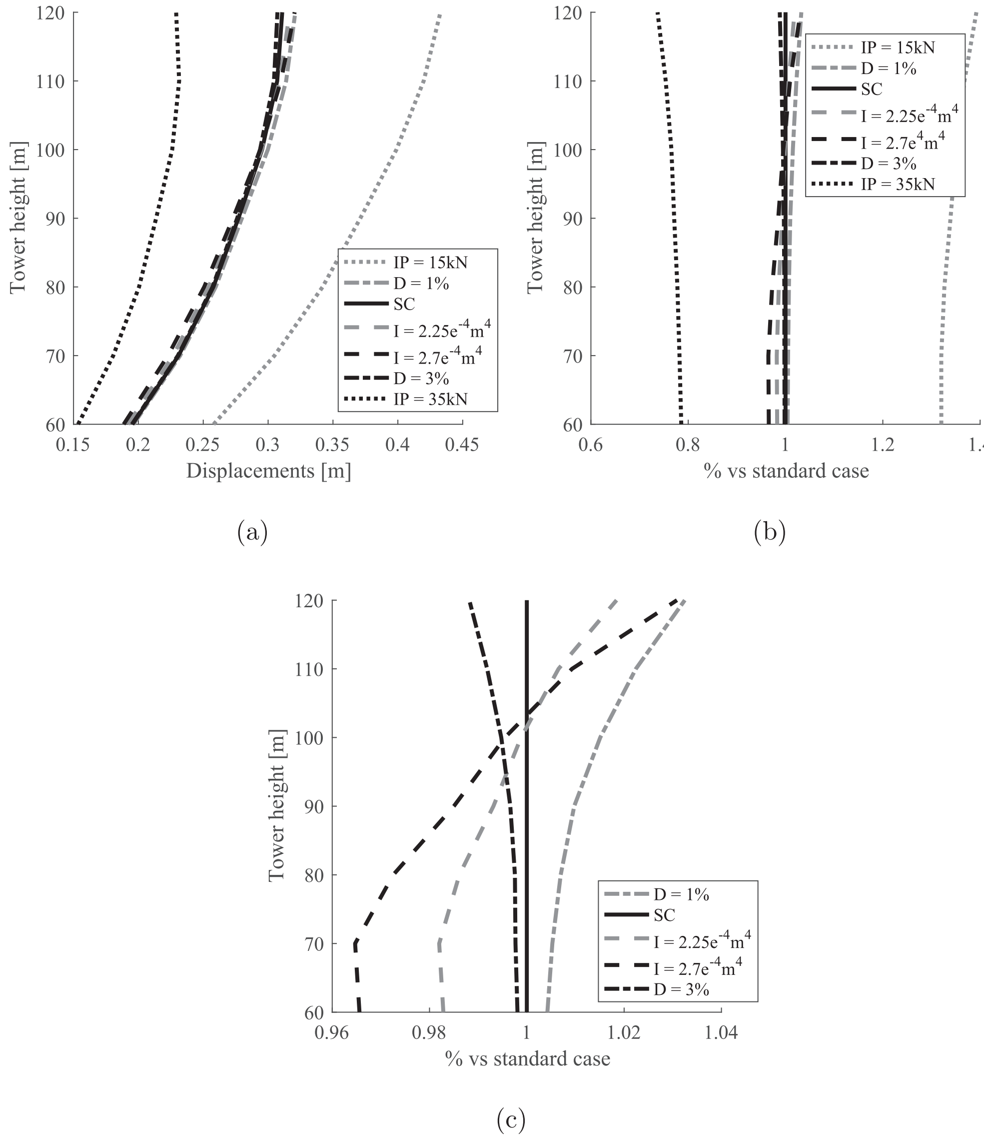

Fig. 11. Guyed mast with WL1. Variation of the 95% probability displacements along the height. a) absolute values of displacements; b) percentage referred to the SC; c) detailed view of the influences of D and I (zoomed (b) plot).

Fig. 12 illustrates the PDF of guy tensions (as percentages of IP), for the guy at level 2 in the *b* direction (cf. Fig. 2) which exhibits the largest values. The shape of the PDFs resembles a Gamma distribution. The highest probable value depicted in the figure exceeds the 240% of IP, for IP = 15 kN, which is the maximum overstress observed in all the studied cases. When IP increases, the PDFs support and dispersion get narrower and the mode also shifts to the left; when IP value is augmented, the variation of tension (referred to IP) during a dynamic event is consistently lower but this trend is nonlinear, specially when the lowest values of IP are compared. The decrease in the variance (and support) of the PDFs as IP increases also indicates that lower values of IP could lead to a higher risk of fatigue. In absolute terms, the maximum value of dynamic cable tension (with extreme low probability), for all the studied cases of IP, never exceeds the 17% σ_u, which provides a good margin of safety for the structural integrity.

Figs. 13 and 14 show similar plots for the guys at levels 3 and 4

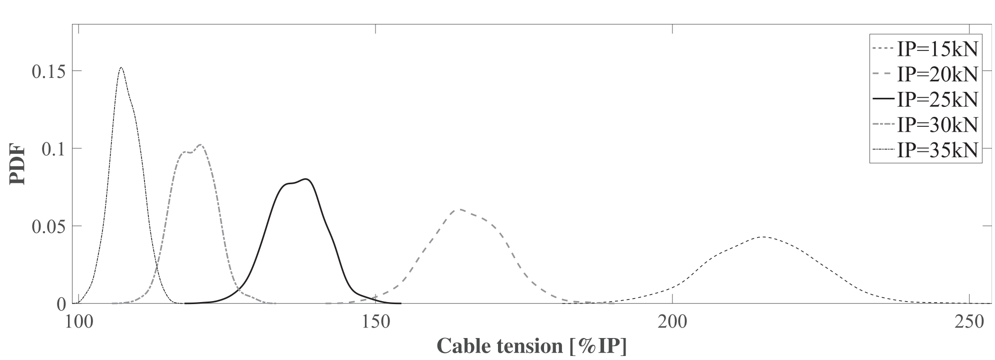

Fig. 12. PDF of guy dynamic tension (as a percentage of IP) for the guys at level 2 and *b* direction.

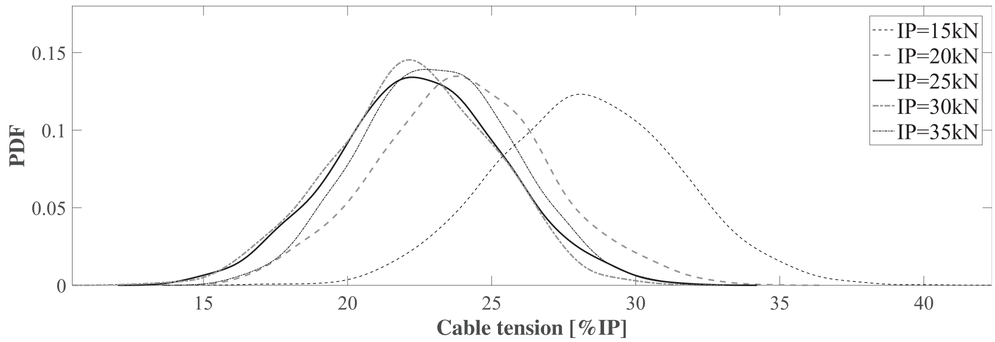

Fig. 13. PDF of guy dynamic tension (as a percentage of IP) for the guys at level 3 and *a* direction.

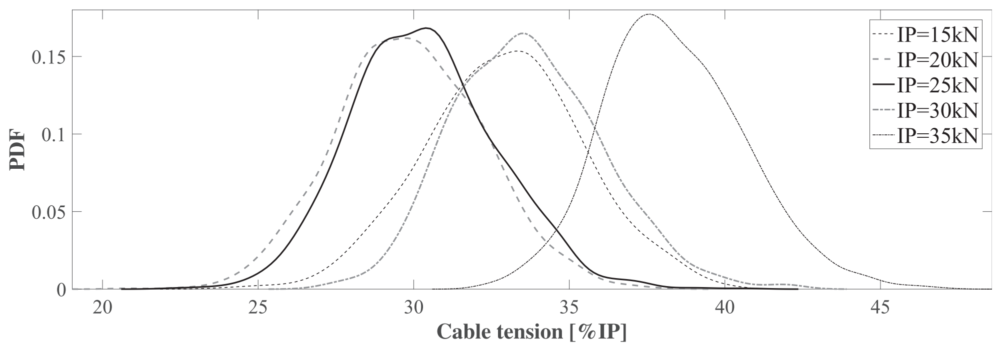

Fig. 14. PDF of guy dynamic tension (as a percentage of IP) for the guys at level 4 w and *a* direction.

respectively, and in the *a* direction (see Fig. 2) which exhibits the lowest values. Again, the shape of the PDFs is Gamma-like. The lowest probable value can be seen in Fig. 13 and it is around the 10% of IP. In Fig. 13, it also can be seen that the IP does not seem to affect the PDF of the results, except for the case of IP = 15 kN which yields higher relative values. The mode location of each PDF depends on IP a nonlinear manner (the grouping of the PDFs does not occur for consecutive values of IP). In general, the loosest guys never lose the 100% of their initial pretension. The presence of a minimum amount of tensile stress must always be checked, to ensure that the truss chains behave as guys.

5. Conclusions

The dynamic nonlinear response of a guyed mast under wind loads was addressed through computational simulations. An analysis of the sensitivity of the structural dynamic response to various parameters was carried out. The parameters considered in the present study were the initial pretension of the guys (IP), the structural damping (D) and the mast bending stiffness (proportional to I). The consequences of using two different approaches to model the wind load are also discussed.

Regarding the loads, the fluctuating component of the wind load WL1 was calculated using the Spectral Representation Method (SRM). This method permits the derivation of a time domain velocity field starting from an adopted power spectral density function of the wind velocity. The obtained signal includes the effect of both the spatial and temporal correlations. Additionally, a simpler wind velocity model constructed as a sum of trigonometric functions (WL2) was used for the sake of comparison.

Several conclusions can be drawn from the study, as listed below:

1. When the dynamic transverse displacements of the mast are analyzed, it is observed that the initial pretension (IP) is, by far, the most important parameter and its influence is nonlinear. The effect is almost constant along the height of the mast.
2. The influence of the mast stiffness (proportional to I) change on the transverse displacements is small (probably due the slenderness of the structure) and variable with the height. Also, larger values of I lead to an increase of the displacements, contrary to the expected behavior.
3. Different values of the Rayleigh damping ratio lead to small changes on the dynamics of the transverse displacements; the effect is variable with the height. It can be concluded that the election of D within the range of values herein studied, is indistinct from a engineering point of view.
4. The transverse displacements found using the simplified wind load WL2 exhibit a periodic behavior, even when the frequency content is in the same range that the one used for WL1 and the amplitude is equivalent. The maximum values of displacement are overestimated and periodic. The study here presented allows to conclude that relevant dynamic characteristics of the wind load that affect the response of the structure, are lost when a simplified approach is used. It is recommended that more complete models of the wind load be used in order to understand and predict more adequately the dynamics of the structure, particularly in the case of important guyed masts.
5 When the lowest value of IP is considered, the maximum and the minimum relative dynamic tensions on the cable are attained, reaching up to 2.5 IP and 0.1 IP, respectively. These extremes are attenuated as IP is increased.

The behaviors described in the previous remarks can have important engineering consequences. Some of the facts could be considered as guidelines in the design and construction of new guyed masts and in the retrofitting of existing structures. In short, they can be summarized as follows. At the design stage, the most important control variable is the initial pretension. During construction, it is relevant to achieve the designed IP value and a proper maintenance program that ensures this tension level during the service life. From the present study, it was found that a decrease in the IP influences negatively and strongly the dynamic response of the mast. In the case of an eventual retrofitting, again the IP variable is the most relevant. That is and in general, it could be preferable to add new cable levels or increase the IP of the existing guys than to reinforce the mast (i.e. to increase I).

Acknowledgments

The authors are grateful for the financial support from the Argentinian agencies Consejo Nacional de Investigaciones Científicas y Técnicas (CONICET, PIP 2014-11220130100007CO), Universidad Nacional del Sur (SGCyT-UNS, PGI-2013 24/J062) and Universidad Tecnológica Nacional (FRM-UTN).

Appendix A. Dynamic wind load

Appendix A.1. Mean component of the wind load

The height dependent mean component of the wind load was designed as a quasi-static wind load, following the Argentinian standard code CIRSOC-INTI (2005). The mean wind load is defined as

$$F = q_z * G * C_f * A_f \tag{A.1}$$

where F is the magnitude of the wind load, G is the gust coefficient, which takes into account the effects of the dynamic amplification and lack of correlation of the loads, for the design of a quasi-static equivalent wind load. Here G is adopted equal to 0.85 which is the lowest value provided by the Argentinian standard and corresponds to fully correlated loads and a non-flexible structure; the lack of correlation will be included in the design of the fluctuating part of the wind load and the effect of the flexibility of the structure is expected to arise naturally from the nonlinear, finite element, dynamic analysis. A_f is the exposed area of the mast, projected onto the plane normal to the loads and C_f is a coefficient which takes into account the shape of the structure, in this case, the mast. Its expression is:

$$C_f = 3,4 * \varepsilon^2 - 4,7 * \varepsilon + 3,4 \tag{A.2}$$

where $\varepsilon = A_f / A_t$ and A_t is the exposed area of the mast without holes. In Eq. (A.1), q_z is the dynamic wind pressure which writes

$$q_z = 0,613 * k_z * k_{zt} * k_d * V^2 * \bar{I} \tag{A.3}$$

where the parameter $\bar{I}$ defines the category of the structure, V is the reference velocity, defined by the location (in this case, the city of Bahía Blanca, Argentina), k_{zt} is the topographic coefficient, k_d is the direction coefficient that takes into account the type of structure (i.e. lattice masts, buildings, etc.) and k_z is a empirical coefficient that considers the load variation with height which is calculated as

$$k_z = 2.01 * (z/z_g)^{2/\alpha} \tag{A.4}$$

z is the height of the considered point, z_g and α are obtained from tables. Table A.2 shows the numerical values adopted or calculated for the coefficients. Figure A.15 shows the load variation along the height and the mean values of the nodal forces applied on the mast.

Table A.2
Coefficients for calculating static wind loads CIRSOC-INTI (2005).

Coefficient	G	A_f	A_t	C_f	I	V	k_d	k_{zt}
Value	0.85	0.57 m^2	9.41 m^2	3.13	1.00	55 m/s	0.85	1

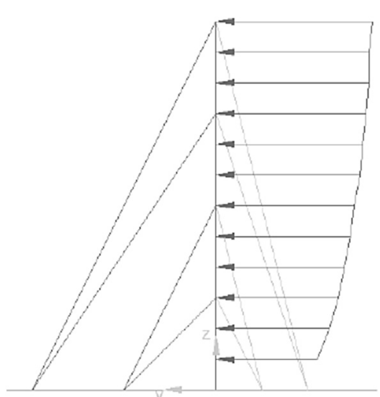

z [m]	Force [N]
10	3320
20	3746
30	4020
40	4226
50	4393
60	4534
70	4658
80	4767
90	4866
100	4956
110	5039
120	5115

Figure A.15. Distribution of mean load in height.

Appendix A.2. WL1: fluctuating part of the wind load through the Spectral Representation Method (SRM)

The fluctuating wind velocity is obtained by the application of the SRM first proposed by Shinozuka and Jan Shinozuka and Jan (1972). The method starts from a power spectral density function (*psdf*) and a coherence function chosen according to the type of problem to be simulated. Then, the random signals are created as a superposition of harmonic functions with a random phase angle, weighed by coefficients that represent the importance of the frequency value within the spectrum and the spatial correlation. Following the methodology, let us first consider a set of *m Gaussian* stationary random processes $f_j^0(t), j = 1, 2, \ldots, m$, with zero mean, $E[f_j^0(t)] = 0$, with a given cross spectral density matrix $S^0(\omega)$ where $S_{jk}^0(\omega) = F[R_{jk(\tau)}^0]$. $F[\ ]$ represents the Fourier Transform operator and $R_{jk}^0(\tau)$ is the cross-correlation function ($j \neq k$) or the autocorrelation function ($j = k$). This matrix verifies $S_{jk}^0(\omega) = \overline{S}_{jk}^0(\omega)$ because, for stationary processes, the correlations matrix verifies $R_{jk}^0(\tau) = R_{jk}^0(-\tau)$ and then, $S^0(\omega)$ results a Hermitian and definite positive matrix. Let $H(\omega)$ denote the lower triangular matrix with Fourier transform, $\overline{H}(\omega)$ its complex conjugate and superscript T, its transpose. If the next decomposition exists

$$S^0(\omega) = H(\omega)\overline{H}^T(\omega), \tag{A.5}$$

it is possible to simulate the process by the following series

$$f_j(t) = \sum_{k=1}^{m}\sum_{n=1}^{N}\left|H_{jk}(w_n)\right|\sqrt{2\Delta\omega}\cos\left[\widehat{\omega}_n t + \theta_{jk}(\omega_n) + \Phi_{kn}\right] \tag{A.6}$$

where $\Delta\omega$ is the frequency interval with which the *psdf* is discretized, $\omega_n = \Delta\omega(n-1)$, $\widehat{\omega}_n = w_n + \psi_{kn}\Delta\omega$, ψ_{kn} is a random value uniformly distributed between 0 and 1, N is the number of frequency intervals and Φ_{kn} are the random independent phase angles that are uniformly distributed between 0 and 2π. If the values of S_{jk} are all real, then the $\theta_{jk}(\omega_n)$ are equal to zero. The decomposition represented by Eq. (A.5) can be found by means of the *Cholesky Decomposition* of the spectral density matrix.

The SRM requires the implementation of different steps. The first one is the adoption of a power spectral density function and a coherence function. In this work, the *psdf* suggested by Davenport is used (*e.g.* refer to Dyrbye and Hansen (1994)):

$$R_N(z,\omega) = \frac{\omega S(z,\omega)}{\sigma^2(z)} = 2/3\frac{f_L^2}{\left(1+f_L^2\right)^{4/3}} \tag{A.7}$$

where ω is the frequency in Hz, σ is the standard deviation and f_L is the nondimensional frequency $f_L = \omega L_u/U(z)$. L_u is the length scale of turbulence (1200 m in Davenport's *psdf*) and $U(z)$ is wind mean velocity at height z. The expression for $U(z)$ corresponds to the potential law adopted by the Argentinian standard, $U(z) = 2.01V(z/z_g)^{2/\alpha}$, V is the wind velocity which, together with z_g and α, are values given by the standard code depending on the characteristics of the structure location. The assumed coherence function is

$$Coh(z_i, z_j, \omega) = exp\left\{-2\omega\frac{C_z|z_i - z_j|}{U(z_i) + U(z_j)}\right\} \tag{A.8}$$

where z_i and z_j are the heights of two given points of the mast. Then, each S_{ij} of the $S(\omega)$ matrix, for a given value of frequency can be calculated as

$$S_{ij}(z_i, z_j, \omega) = \sqrt{S(z_i,\omega)S(z_j,\omega)}\ Coh(z_i, z_j, \omega) \tag{A.9}$$

Following this procedure, N matrices are created, one for each value of the frequency. Next, these matrices should be transformed in order to find the $H(\omega)$ matrices. Now, it is possible to construct the temporal series given by

$$u(z_j, t) = \sum_{k=1}^{m}\sum_{n=1}^{N} H_{jk}(\omega_n)\sqrt{2\Delta\omega}\cos[2\pi\widehat{\omega}_n t + \Phi_{kn}] \tag{A.10}$$

The data used to construct the fluctuating part of the wind velocity are depicted in Table A.3.

Table A.3
Coefficients used to calculate the time dependent velocity field.

Coefficient	σ^2	L_u	C_z	ω_c	$\Delta\omega$	Δt	N	m
Value	38.77	1200 m	11.5*	2.5 Hz	0.004 Hz	0.2 s	625	12

Appendix A.3. WL2: simple model for the fluctuating part of the wind load

As a simpler alternative, the temporal variation function is represented as a sum of cosine functions using frequencies extracted from the peak zone of the Davenport's *psdf*, following the expression:

$$F(t) = \overline{F}\left(1 + 0.4\sum_{i=1}^{n} cos(2\pi\omega_i t)\right) \tag{A.11}$$

where $\overline{F}$ is the mean component of the wind load, calculated using the Argentinian Standard CIRSOC-INTI (2005) procedures. The frequency content varies slightly with the height (following the variation of the reference wind velocity) and then, the time variation of each nodal load is slightly different. As a reference, at the top of the mast, the frequencies used to construct the harmonic load were $\omega_i \in [0.11 : 0.01 : 0.19]$ Hz. Unlike the load case WL1, neither spatial nor temporal correlations are considered in this harmonic function. A 40% of the mean value of the nodal force is taken as the maximum amplitude of the dynamic action.

References

American Society of Civil Engineers, 1998. Minimum Design Loads for Building and Other Structures-ASCE 7-98. ASCE, New York, USA.
ANSI/TIA-222-G, 2009. Structural Standard for Antenna Supporting Structures and Antennas, ANSI/TIA-222-G. Telecommunications Industry Association.
ALGOR V23.01. Professional MES, 2009. Autodesk Inc., Pittsburg, USA.
CIRSOC-INTI, 2005. Reglamento CIRSOC 102. Acción del Viento sobre las Construcciones. INTI, Buenos Aires, Argentina.
CIRSOC-INTI, 2008. Proyecto de Reglamento Argentino para Construcciones Sismorresistentes Parte 1. Construcciones en General. INTI, Buenos Aires, Argentina.
Clough, R., Penzien, J., 1993. Dynamics of Structures. McGraw-Hill, New York.
de Oliveira, M.I., da Silva, J.G., Vellasco, P. C. da S., de Andrade, S.A., de Lima, L.R., 2007. Structural analysis of guyed steel telecommunication towers for radio antennas. J. Braz. Soc. Mech. Sci. Eng. 29, 185–195.
Desai, Y., Punde, S., 2001. Simple model for dynamic analysis of cable supported structures. Eng. Struct. 23, 271–279.
Dyrbye, C., Hansen, S., 1994. Wind Loads On Structures, first ed. John Willey and Sons, West Sussex, England.
Harikrishna, P., Annadurai, A., Gomathinayagam, S., Lakshmanan, N., 2003. Full scale measurements of the structural response of a 50 m guyed mast under wind loading. Eng. Struct. 25, 859–867.
International Association for Shell and Spatial Structures, 1991. Recommendation for the Design and Analysis of Lattice Towers. IASS, Madrid, España.
Kahla, N.B., 1993. Equivalent beam-column analysis of guyed towers. Comput. Struct. 55 (4), 631–645.
Kewaisy, T.H., 2001. Nonlinear Dynamic Interaction between Cables and Mast of Guyed-tower Systems Subjected to Wind-induced Forces. Ph.D. thesis. Texas Tech University.
Lu, L., Qu, W., Li, M., 2010. Simulation of wind velocity and calculation of wind load for guyed masts, Wuhan Ligong Daxue Xuebao (Jiaotong Kexue Yu Gongcheng Ban). J. Wuhan Univ. Technol. Transp. Sci. Eng. 34, 1057–1060.
Madugula, M., Wahba, Y., Monforton, G., 1998. Dynamic response of guyed masts. Eng. Struct. 20 (12), 1097–1101.
Meshmesha, H., Sennah, K., Kennedy, J.B., 2006. Simple method for static and dynamic analyses of guyed towers. Struct. Eng. Mech. 23 (6), 635–649.
Preidikman, S., Massa, J., Roccia, B., 2006. Análisis dinámico de mástiles arriostrados. Rev. Int. de Desastres Nat. Accid. e Infraestructura Civ. 6 (1), 85–102.
Saudi, G., 2014. Structural assessment of a guyed mast through measurement of natural frequencies. Eng. Struct. 59, 104–112.
Shi, H., 2007. Nonlinear Finite Element Modeling and Characterization of Guyed Towers under Severe Loading. Ph.D. thesis. University of Missouri, Columbia.
Shinozuka, M., Jan, C., 1972. Digital simulation of random processes and its applications. J. Sound Vib. 25 (1), 111–128.
Venanzi, I., Materazzi, A.L., Ierimonti, L., 2015. Robust and reliable optimization of wind-excited cable-stayed masts. J. Wind Eng. Ind. Aerodyn. 147, 368–379.
Wahba, M., Madugula, M., Monforton, G., 1998. Evaluation of non-linear analysis of guyed antenna towers. Comput. Struct. 68, 207–212.